Available online at www.sciencedirect.com
ScienceDirect
Ceramics International 37 (2011) 555–560
CERAMICS INTERNATIONAL
www.elsevier.com/locate/ceramint

Effect of doping concentration on the properties of aluminium doped zinc oxide thin films prepared by spray pyrolysis for transparent electrode applications

C.M. Muiva *, T.S. Sathiaraj, K. Maabong

Physics Department, University of Botswana, P/Bag, 0022, Gaborone, Botswana

Received 9 January 2010; received in revised form 21 September 2010; accepted 24 September 2010
Available online 28 October 2010

Abstract

Zinc oxide possesses many interesting properties, such as modifiable conductivity, wide band gap, high excitonic binding energy, piezo-electric polarisation and cathodoluminiscence. In this study transparent conducting aluminium doped zinc oxide (ZnO:Al) thin films were deposited on float glass substrates by tailor made spray pyrolysis with adaptation for measuring the actual temperature of the substrate surface during deposition. The films were characterised and the effect of aluminium doping concentration [Al/Zn] on their optical, electrical and structural properties was investigated as a function of aluminium doping between 0 and 10 at.%. There was widening of optical band gap with increasing doping concentration. ZnO:Al films with low resistivity of 2.8×10^{-2} Ω cm and high transmittance of over 85% at 550 nm which are crucial for opto-electrical applications were obtained at a doping ratio of 2 at.%.

Keywords: A: Thin films; D: ZnO; Spray pyrolysis

1. Introduction

In the last decade, zinc oxide thin film has attracted much attention due to its interesting properties such as high resistance to chemical attack, thermal stability, stability in hydrogen plasma commonly used in the fabrication of amorphous silicon solar cells, non toxicity and good adherence to many substrates. High optical transparency in the visible region, wide band gap and the high refractive index of 1.8 enables several applications including antireflection coating in solar cells industry [1], heat mirrors and multilayer photo thermal conversion systems [2]. Low resistivity has enabled applications as transparent electrodes for solar cells, liquid crystal displays (LCD) and organic light emitting diodes (LED) [3]. ZnO is a piezo-electric material and has been applied in surface acoustic wave devices and piezo-electric transducers [4]. Change in resistivity on exposure to certain gaseous materials has enabled use in solid state gas sensing devices [5]. Its abundance in nature and non-toxicity makes it an attractive material when compared with indium tin oxide (ITO) and cadimium tin oxide (Cd_2SnO_4) [6].

Many techniques have been previously used to deposit ZnO/ZnO:Al films on different substrates. These include filtered vacuum arc [7], sol–gel process [8], spray pyrolysis technique (SPT) [9], chemical vapour deposition (CVD) [10], pulsed laser deposition [11], molecular beam epitaxy (MBE) [12], electro-deposition [13], electron beam evapouration [14], chemical-bath deposition (CBD) [15] and sputtering [16]. Compared to other thin film deposition techniques, SPT offers advantage of use of inexpensive equipment (non vacuum method), ease of large scale adoption by moving nozzle over a large substrate and possibility of microprocessor based spraying which is useful tool in electronics. In SPT, there is easy control of roughness leading to light scattering which is a useful tool in solar cells and ease of tailoring of film properties for desired application by changing deposition and post deposition conditions. Resistivity of sprayed doped ZnO has arrived at a stage of favourable comparison with those from other well established deposition techniques such as sputtering [17].

The prime requisite for obtaining good quality sprayed thin film is the optimisation of preparative conditions. These are:

* Corresponding author. Tel.: +267 355 2618; fax: +267 318 5097.
E-mail address: cmuiva@yahoo.co.uk (C.M. Muiva).

0272-8842/$36.00
doi:10.1016/j.ceramint.2010.09.042

substrate temperature, spray rate, concentration of solution, spray rate, type and pressure of the carrier gas, the geometric characteristics of the spray system etc. Generally, in a spray pyrolysis process, reaction temperature is a basic operating variable and as such optimisation of the actual surface temperature of the substrate during the spray cycle is paramount. In addition, solution properties such as precursor composition, concentration, or the addition of a co-solvent may be crucial to achieve the desired product composition and morphology [18,19]. For opto-electrical applications, defects population control and carrier multiplication through doping are crucial for low resistivity. Considering the numerous studies done on aluminium doped zinc oxide by spray pyrolysis technique, and to our knowledge, the aluminium doping does not exceed a few at.%. In this study we thought it would be important to study the electrical, optical and micro-structural properties of the sprayed ZnO at high Al doping concentration.

2. Experimental procedure

Aluminium doped zinc oxide thin films (ZnO:Al) were deposited onto 3 cm × 7 cm float glass substrates by spray pyrolysis using a homemade spraying equipment. The starting solution was 0.2 M zinc acetate prepared by dissolving the equivalent mass of zinc acetate in a mixture of deionised water and methanol, in the ratio of 35:65, respectively. A few drops of acetic acid were added to stabilise the solution and prevent precipitation of zinc hydroxide. Aluminium pentanedionate was added to the zinc acetate during preparation of the solution for doping such that the doping concentration in the starting solution was between 0 and 10 at.%. The concentration of dopant in the starting solution was found to be within 4–9% of the actual value of the dopant incorporated in the films as confirmed from standardised EDX studies. Nitrogen gas of purity 99.8% was used as a carrier gas and was allowed to flow out through a pipe with its end fitted with a fine glass nozzle of ∼1.5 mm diameter. The solution was drawn by a pipe with a fine nozzle (∼0.5 mm) at the end from a calibrated vessel that was placed on top of an ultrasonic generator to ensure that there was homogeneous mixing of the solution throughout the spraying session. The spray rate used for all samples was 2.0 ml/min.

The substrates were heated by a Philips Harris 1100 hotplate heater. A bimetallic thermometer that could measure the temperature to an accuracy of ±5 °C was used to measure the temperature. Control experiments were set up to monitor the temperature of the substrate surface in contact with the droplets during actual deposition as it was found to be lower than the backside of the substrate in contact with the heater. For all the samples the substrate was placed 28 cm below the nozzle and the substrate temperature was 420 °C.

The thickness of the films was measured using a P-15 KLA Tencor stylus surface profiler. The optical transmittance and reflectance for all wavelengths in the range of $300 < \lambda < 3000$ nm (to an accuracy of ±0.1 nm in the UV–vis and 0.4 nm in the NIR) were measured using a Cary 500 scan UV/VIS/NIR spectrophotometer. A four point probe equipped with two Keithley 197 Autoranging Microvolt DMM meters for measuring voltage and current, an EZ GP-4303 power supply and a Signatone probing table was used for electrical measurements. In this study the morphology of the films was studied by using X-ray diffraction data obtained from a Philips 3710 X-ray diffraction (XRD) system. The radiation used was cu-Kα 1 with a wavelength of 1.54056 Å within the values of 2θ between 5.01–74.9°. The surface of the films was studied using a XL 30 ESEM scanning electron microscope. The elementary composition of the films was determined from results obtained from Energy Dispersive Analysis of X-rays (EDAX).

3. Results and discussion

3.1. Structural properties

For hexagonal wurtzite structure, the lattice parameters, a (the second nearest neighbour distance) and c (the length of bond parallel to c-axis) are related to d spacing and the miller indices h, k and l through the expression [20];

$$\frac{1}{d^2} = \frac{4}{3}\left(\frac{h^2 + hk + l^2}{a^2}\right) + \frac{l^2}{c^2} \quad (1)$$

where d is the interplanar spacing which is obtained from Bragg's law, and h, k and l are the Miller indices denoting the plane. For (0 0 2) peak h, k and l are 0, 0 and 2 respectively and for (1 0 1) peak are 1, 0 and 1 respectively. An estimation of the averaged crystallite size has been done using the well known formula of Deby–Scherrer [21]:

$$D = \frac{0.9\lambda}{\beta\cos\theta} \quad (2)$$

where β is the observed angular width at half maximum intensity (FWHM) of the peak; λ, is the X-ray wavelength (1.5406 Å for Cu Ka1) and θ is the Bragg's angle. Table 1 summarises the values of structural parameters of ZnO thin films fabricated using different concentrations of Al dopant in the starting solution.

Results presented in Fig. 1 shows that the grain sizes decreased with increase in the concentration of aluminium in the starting solutions from 41.618 nm at 0 at.% to 19.818 nm at 6 at.% doping. This decrease is correlated by broadening of the XRD pictographs as indicated by corresponding increase in the FWHM values. The intensity of the (0 0 2) peak decreases as the

Table 1
Grain sizes and lattice parameters of ZnO thin films fabricated using different concentrations of Al dopant in the starting solution at a substrate temperature of 420 °C and a solution flow rate of 2.0 ml/min.

% of Al	d (Å)	2θ (0 0 2) peak	Grain size (nm)	c (Å)	a (Å)	$\mu = c/a$
0	2.594	34.544	41.618	5.189	3.459	1.500
1	2.601	34.459	32.006	5.201	3.467	1.500
2	2.590	34.599	26.014	5.181	3.454	1.500
3	2.591	34.632	32.021	5.182	3.455	1.500
4	2.588	34.632	35.707	5.176	3.451	1.500
5	2.583	34.703	19.826	5.166	3.444	1.500
6	2.594	34.549	19.818	5.188	3.459	1.500
10	2.799	No peak				

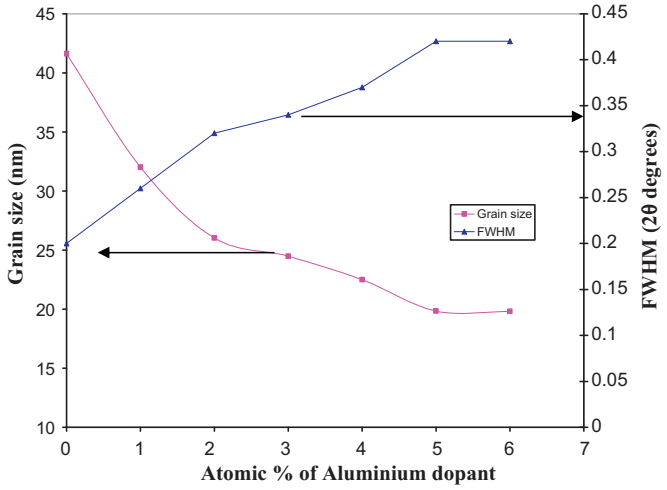

Fig. 1. Grain size and FWHM as a function of aluminium doping concentration.

concentration of aluminium increases as shown in Fig. 2 which is possibly due to segregation of Al_2O_3 into the grain boundaries [22] which inhibits the growth of the particle size in the films as the Al concentration increases. It can be observed that for pure undoped and lightly doped (<2 at.%) ZnO films, the most predominant peak is the (0 0 2) peak. The (1 0 0) and (1 0 1) peaks are far smaller compared to the (0 0 2) peak indicating preferred orientation along the *c*-axis perpendicular to the substrate surface.

As the aluminium concentration increases, the (1 0 0) and (1 0 1) start to appear and the (0 0 2) peak becomes smaller and no (0 0 2) peaks were observed in 10 at.% doped films, showing total diversion from growth with *c*-axis perpendicular to the substrate surface to other orientations. This shows that increase in aluminium concentration leads to random orientation. A similar trend was observed by EI Manounia et al. [23] and Nunesa et al. [24] for the doping range of 1–4 at.% and 1–5 at.%, respectively at substrate temperature of 400 °C. So the variation in the preferential orientation can be obviously accounted for in terms of the increase of the surface energy density above a critical Al doping concentration. That is why with different orientations nucleations are able to increase for Al doping concentration greater than 2 at.%. It can be concluded that the amount of doping modifies the film growth process and consequently the microstructure. Hence the decrease in the intensity of (0 0 2) preferential orientation may indicate a meaningful increase of staking defects and a loss of periodicity in the arrangement of ZnO crystals.

The variations in positions of the (0 0 2) peak intensity as a function of Al concentration are observed in Fig. 3. A small deviation in the (0 0 2) peak was found when the concentration was varied, indicating that some residual stress inside the film may exist. Jeong et al. [25] observed an increase in the position of the (0 0 2) peak with increased doping and attributed this shift of the (0 0 2) diffraction peak position from its normal value to residual stress in the film caused by the difference in ionic sizes between Zn^{2+} (72 pm) and Al^{3+} (53 pm). They observed that increased doping with ions Ag^{+} (122 pm) larger than Zn^{2+} led to a decrease in position of the peaks. This is confirmed by lattice parameters, *a* and *c*, which are less than the bulk which is a strong indication of stress in the films.

3.2. Optical properties

Fig. 4 shows the optical transmission spectra of zinc oxide films prepared on glass substrate at substrate temperature of 420 °C for different aluminium doping concentrations. All films irrespective of the doping concentration employed are highly transparent in the visible range (400–750 nm) of the optical spectrum, reaching values up to 85% at 550 nm. It is worth noting here that the obtained layers will give satisfactory optical window in visible range for optical applications. The decrease of transmittance at higher doping levels (>2 at.%) after 700 nm may be attributed to the increased scattering of photons by crystal

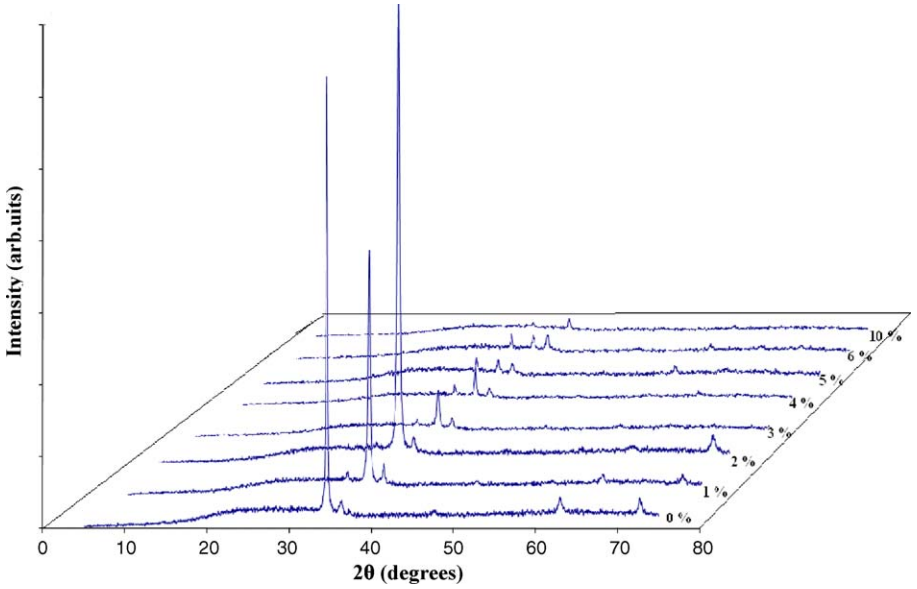

Fig. 2. XRD peak intensities of films prepared at different ratios of aluminium doping in the starting solution for ZnO:Al thin films.

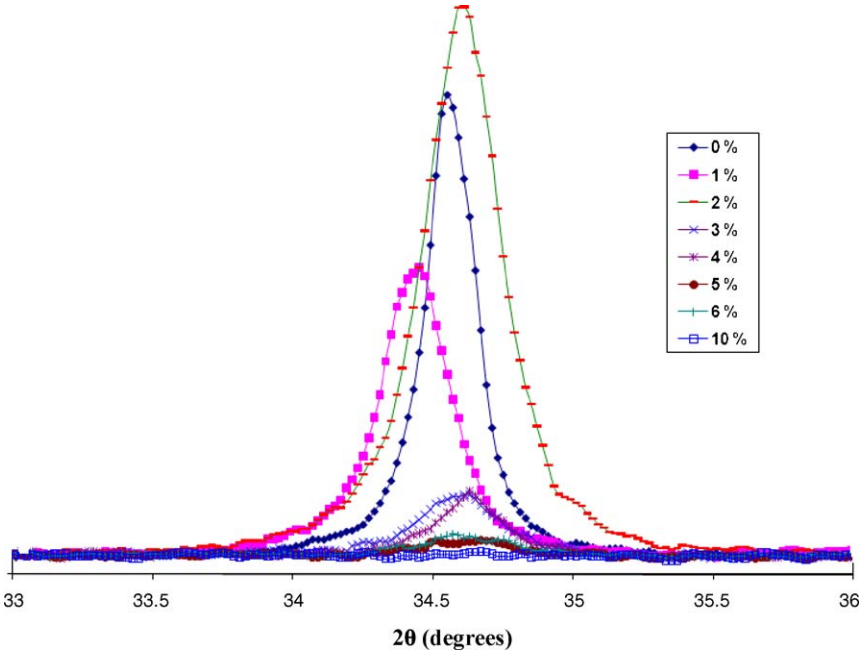

Fig. 3. XRD peak position as a function of aluminium dopant concentration.

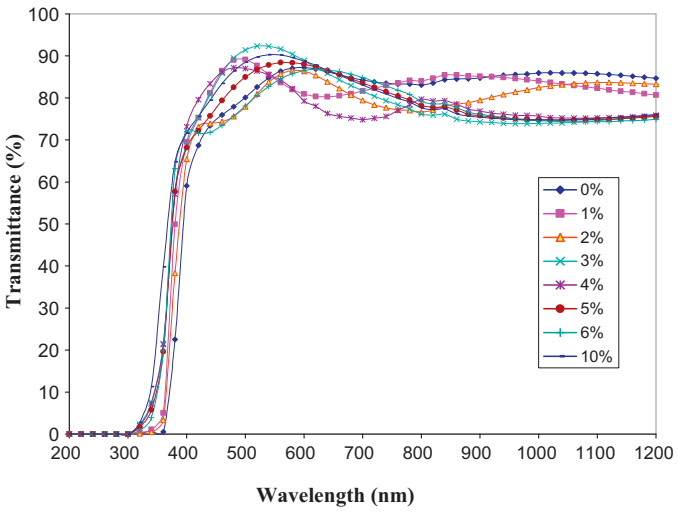

Fig. 4. Transmittance spectra of films prepared at different atomic ratios of aluminium in the starting.

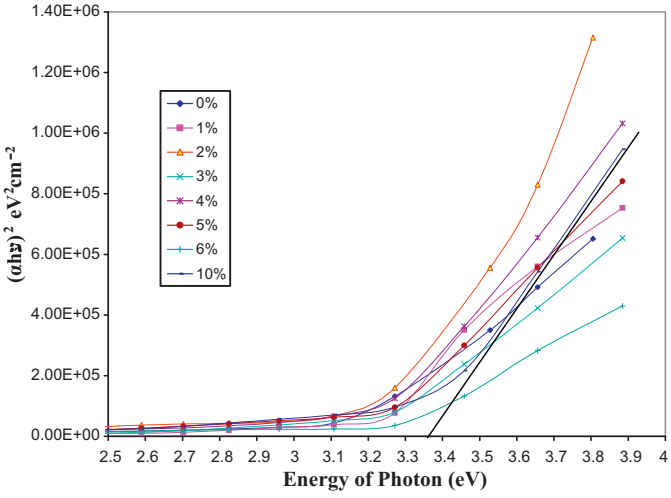

Fig. 5. Plot of $(\alpha h\nu)^2$ and energy of the incident photon for films prepared at different aluminium doping concentration in the starting solution. A method for obtaining the band gap has been illustrated for one of the samples.

defects created by doping [26]. The free carrier absorption of the photons may also contribute to the observed reduction in the optical transmission of heavily doped films.

According to theoretical and practical results, ZnO exhibits direct inter band transitions [27] and for allowed direct transitions between parabolic bands, the variation of absorption coefficient, α with photon energy ($h\nu$) was found to obey the relation [28];

$$\alpha h\nu = A(h\nu - E_g)^{1/2} \quad (3)$$

where $h\nu$ is photon energy, α is the absorption coefficient, A is a constant and E_g is the band gap. From Eq. (3) it follows that,

$$(\alpha h\nu)^2 = A(h\nu - E_g) \quad (4)$$

Plotting $(\alpha h\nu)^2$ against photon energy $h\nu$, the band gap value can be determined by extrapolating the straight line portion at $\alpha = 0$ as indicated for one of the plots in Fig. 5. In Fig. 5, a presentation of the plots of $(\alpha h\nu)^2$ values and energy of incident radiation are made. The values of band-gap energy, E_g of doped ZnO thin films for different doping rates were then obtained by extrapolation method. It was observed that as the Al content increases, the absorption edge shifts in monotonously to a higher energy region from 3.18 eV to 3.23 eV for the undoped and 1 at.% respectively, to 3.35 eV for 10 at.% doped films. This agrees with other workers [29], for increasing aluminium doping concentration. This broadening effect is due to the Burstein- Moss effect, which implies an increase in the Fermi level in the conduction

band of semiconductors due to increased carriers, leading to widening of the optical band-gap.

3.3. Electrical properties

Fig. 6 is the plot of resistivity against percentage of Al dopant. A near parabolic behaviour with a minimum is observed. It can be observed that the resistivity decreased from 2.02 Ω cm for a doping of 1 at.% to a minimum of 2.8×10^{-2} Ω cm for films prepared with a starting solution containing 2 at.%. The resistivity then started increasing with doping concentration to 6.67×10^{-1} Ω cm at 6 at.% doping. This shows that the resistivity reaches a minimum at 2 at.% Al doping. This result is quite comparable to other reports [24,30,31,32] for sprayed ZnO:Al films for similar substrate temperature and doping range. When a small amount of Al was introduced into the ZnO film, the Al was ionised into Al^{3+} and substituted for Zn^{2+}. Thus, one free electron was produced from one zinc atom replaced by an aluminium atom. Small amounts of aluminium introduce large numbers of free electrons in the doped films, and the conductivity therefore increases. But further increase of aluminium concentration (>2 at.%) does not further increase the conductivity. Excess amount of aluminium cannot be accommodated into ZnO lattice due to its limited solid solubility and therefore form neutral aluminium oxide and segregates in the grain boundaries [33]. Therefore, the amount of electrically active Al atoms in the film is reduced when the Al doping is high and excess dopant lead to build up of carrier traps in the lattice reducing their mobility. In the case of the films deposited with the optimum [Al]/[Zn] ratio (2 at.%), we suppose the solubility limit of Al into ZnO lattice is reached hence Al is uniformly distributed inside the grains and a continuous film is obtained, and consequently the electrical resistivity reaches its minimum value. Resistivity of sprayed ZnO thin films is known to decrease with increasing film thickness [34]. Increased film thickness leads to better stacking of the film with resultant increase in grain size thus reducing grain defects and grain boundary scattering [35] which have negative effects on carrier mobility. Considering that our films were kept less than 1 μm thick as a trade off for transmittance which is lower for thicker films, the resistivity may have been higher than the current minimum values reported in literature.

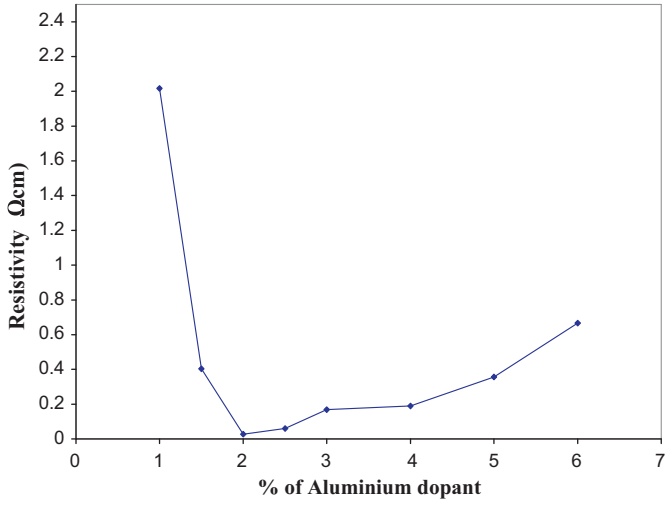

Fig. 6. Resistivity as a function of Al doping concentration for ZnO: Al films.

4. Conclusion

Quality ZnO:Al thin films were prepared by spray pyrolysis starting from Zinc acetate and aluminium pentanedionate as sources of ZnO and Al respectively. From the results, the transmittance in the visible range was found to be above 80%. The lowest resistivity was 2.4×10^{-2} Ω cm for a doping of 2 at.%. X-ray diffraction studies showed that the films grown at optimum conditions are polycrystalline with preferred (0 0 2) orientation and the peaks fit well to the hexagonal wurtzite structure. There was a decrease in grain size from 41.62 nm at 0 at.% aluminium doping concentration, to 19.82 nm at 6 at.%. In all cases the lattice parameters were found to be less than the bulk values due to stress in the film. The optical band gap increases with doping concentration from 3.18 eV to 3.35 eV for the doping concentration increase from 0 at.% to 10 at.%. The properties of films produced at optimum conditions are suitable for optical and electrical applications owing to their low resistivity, high optical transmittance in the visible range and very low transmittance in the UV region.

References

[1] O. Kluth, B. Rech, L. Houben, S. Wieder, G. Schöpe, C. Beneking, H. Wagner, A. Löffl, H.W. Schock, Texture etched ZnO:Al coated glass substrates for silicon based thin film solar cells, Thin Solid Films 351 (1999) 247–253.

[2] Z.-C. Jin, I. Hamberg, C.G. Granqvist, B.E. Sernelius, K.-F. Berggren, Reactively sputtered ZnO: Al films for energy-efficient windows, Thin Solid Films 164 (1988) 381–386.

[3] J. Yoo, J. Lee, S. Kim, K. Yoon, I. Jun Park, S.K. Dhungel, B. Karunagaran, D. Mangalaraj, Y. Junsin, High transmittance and low resistive ZnO:Al films for thin film solar cells, Thin Solid Films 480–481 (2005) 213–217.

[4] T. Shiosaki, M. Adachi, A. Kawabata, Piezoelectric thin films for SAW applications, Thin Solid Films 96 (1982) 129–140.

[5] T. Sergiu, S. Teodor, I. Shishiyanu, Oleg Lupan, Sensing characteristics of tin-doped ZnO thin films as NO_2 gas sensor, Sens. Actuators B 107 (2005) *379*–386.

[6] R.G. Gordon, Criteria for choosing transparent conductors, MRS Bull. 25 (8) (2000) 52–57.

[7] T. David, S. Goldsmith, R.L. Boxman, Electro-optical and structural properties of thin ZnO films prepared by filtered vacuum arc deposition, Thin Solid Films 447–448 (2004) 61–67.

[8] Z. Hong-ming, Y. Dan-qing, Y. Zhi-ming, X. Lai-rong, L. Jian, Preparation of aluminum doped zinc oxide films and the study of their microstructure, electrical and optical properties, Thin Solid Films 515 (17) (2007) 6909–6914.

[9] A. El Manounia, F.J. Manjona, M. Peralesa, M. Mollara, B. Maŕa, M.C. Lopez, J.R. Barradoc, Effect of thermal annealing on ZnO:Al thin films grown by spray pyrolysis, Superlattices Microstruct. 42 (2007) 134–139.

[10] D. Kim, I. Yun, H. Kim, Fabrication of rough Al doped ZnO films deposited by low pressure chemical vapor deposition for high efficiency thin film solar cells, Curr. Appl. Phys. (2010), doi:10.1016/j.cap.2010.02.030.

[11] H Kim, J.S. Horwitz, W.H. Kim, A.J. Mäkinen, Z.H. Kafafi, D.B. Chrisey, Thin Solid Films 420–421 (2002) 539–543.
[12] K. Nakahara, H. Takasu, P. Fons, A. Yamada, K. Iwata, K. Matsubara, R. Hunger, S. Niki, Growth of N-doped and Ga + N-codoped ZnO films by radical source molecular beam epitaxy, J. Cryst. Growth 237–239 (2002) 503–508.
[13] J.S. Wellings, A.P. Samantilleke, P. Warren, S.N. Heavens, I.M. Dharmadasa, Comparison of electrodeposited and sputtered intrinsic and aluminium-doped zinc oxide thin films, Semicond. Sci. Technol. 23 (2008) 125003–1250010.
[14] D.R. Sahu, S. Lin, J. Huang, Investigation of conductive and transparent Al-doped ZnO/Ag/Al-doped ZnO multilayer coating by electron beam evapouration, Thin solid films 516 (2008) 4728–4732.
[15] S.T. Shishiyanu, O.I. Lupan, E.V. Monaico, V.V. Ursaki, T.S. Shishiyanu, I.M. Tiginyanu, Photoluminescence of chemical bath deposited ZnO:Al films treated by rapid thermal annealing, Thin Solid Films 488 (2005) 15–19.
[16] C. Guillén, J. Herrero, High conductivity and transparent ZnO:Al films prepared at low temperature by DC and MF magnetron sputtering, Thin Solid Films 515 (2) (2006) 640–643.
[17] K. Ellmer, Magneteron sputtering of transparent conductive zinc oxide: relation between the sputtering parameters and the electronic properties, J. Phys. D: Appl. Phys. 33 (2000) R17–R32.
[18] A.C. Tickle, Thin Film Transistors, John Wiley and Sons, New York, USA, 1969.
[19] E. Bacaksiz, M. Parlak, M. Tomakin, A. Özçelik, M. Karakız, M. Altunbaş, The effects of zinc nitrate, zinc acetate and zinc chloride precursors on investigation of structural and optical properties of ZnO thin films, J. Alloys Compd. 466 (2008) 447–450.
[20] B.E. Warren, X-ray diffraction, Dover New-York (1990) p.253.
[21] B.D. Cullity, S.R. Stock, Elements of X-Ray Diffraction, Third Ed., Prentice-Hall, New York, 2001, p. 99.
[22] S.B. Majumder, M. Jain, P.S. Dobal, R.S. Katiyar, Investigations on solution derived aluminium doped zinc oxide thin films, Mater. Sci. Eng. B 103 (2003) 16–25.
[23] A. El Manounia, F.J. Manjónb, M. Mollar, B. Maríb, R. Gómez, M.C. López, J.R. Ramos-Barradod, Effect of aluminium doping on zinc oxide thin films grown by spray pyrolysis, Superlattices Microstruct. 39 (2006) 185–192.
[24] P. Nunesa, E. Fortunatoa, P. Tonelloa, F. Braz Fernandesa, P. Vilarinhob, R. Martins, Effect of different dopant elements on the properties of ZnO thin films, Vacuum 64 (2002) 281–285.
[25] S.H. Jeong, B.N. Park, S.B. Lee, J.H. Boo, Metal-doped ZnO thin films, synthesis and characterisations, Surf. Coat. Technol. 201 (2007) 5318–5322.
[26] B. Joseph, P.K. Manoj, V.K. Vaidyan, Studies on the structural, electrical and optical properties of Al-doped ZnO thin films prepared by chemical spray deposition, Ceram. Int. 32 (2006) 487–493.
[27] E.C Etiñorğu, S. Goldsmith, Chemical and thermal stability of the characteristics of filtered vacuum arc deposited ZnO, SnO_2 and zinc stannate thin films, J. Phys. D: Appl. Phys. 40 (2007) 5220–5236.
[28] Y. Ohta, Y. Haga, Y. Abe, Crystallographic features of ZnO single crystals, Jpn. J. Appl. Phys. 36 (1997) L1040–L1042.
[29] A.F. Akta Ruzzuman, G.L. Sharma, L.K. Malhotra, Electrical, optical and annealing characteristics of ZnO:Al films prepared by spray pyrolysis, Thin solid films 198 (1–2) (1991) 67–74.
[30] F Kadi Allah, S. Yapi Abé, C.M. Núñez, A. Khelil, L. Cattin, M. Morsli, J.C. Berne'de, A. Bougrine, M.A. del Valle, F.R. Díaz, Characterisation of porous doped ZnO thin films deposited by spray pyrolysis technique, Appl. Surf. Sci. 253 (2007) 9241–9247.
[31] H. Mondragón-Suárez, A. Maldonado, M. de la, L. Olvera, A. Reyes, R. Castanedo-Pérez, G. Torres-Delgado, R. Asomoza, ZnO:Al thin films obtained by chemical spray: effect of the Al concentration, Appl. Surf. Sci. 193 (1–4) (2002) 52–59.
[32] H. Lee, B. Park, Characteristics of Al-doped ZnO thin films obtained by ultrasonic spray pyrolysis: effects of Al doping and an annealing treatment, Mater. Sci. and Eng., B 103 (3) (2004) 242–245.
[33] H. Gomez-Pozos, A. Maldonado, M de la L. Olver, Effect of the [Al/Zn] ratio in the starting solution and deposition temperature on the physical properties of sprayed ZnO:Al thin films, Mater. Lett. 61 (2007) 1460–1464.
[34] Z.B. Achour, T. Ktari, B. Ouertani, O. Touayar, B. Bessais, J.B. Brahim, Effect of doping level and spray time on zinc oxide thin films produced by spray pyrolysis for transparent electrodes applications, Sens. Actuators A 134 (2007) 447–451.
[35] X. Yu, J. Ma, F. Ji, Y. Wang, C. Cheng, H. Ma, Thickness dependence of properties of ZnO:Ga films deposited by RF magnetron sputtering, Appl. Surf. Sci. 245 (2005) 310–315.